in a five-coordinate complex is not a good model to compare with the six-coordinate O_2 adduct to infer Co(III)–O_2^-.

(16) D. Getz, E. Melamud, B. L. Silver, and Z. Dori, *J. Am. Chem. Soc.*, **97**, 3846 (1975), and references therein.

(17) (a) G. A. Rodley and W. T. Robinson, *Nature* (*London*), **235**, 438 (1972); (b) L. D. Brown and K. N. Raymond, *Inorg. Chem.*, **14**, 2590 (1975), and references therein; (c) D. H. Templeton, C. H. Dauben, *J. Am. Chem. Soc.*, **72**, 2251 (1950); (d) G. S. Zhdanov and Z. V. Zvonkova, *Dokl. Akad. Nauk. SSSR*, **82**, 743 (1952); (e) R. J. Celotta et al., *Phys. Rev. A*, **6**, 631 (1972).

(18) M. Israel, J. S. Rosenfield, and E. J. Modest, *J. Med. Chem.*, 7, 710 (1964).

(19) L. Sacconi and I. Bertini, *J. Am. Chem. Soc.*, **88**, 5180 (1966).

(20) R. H. Niswander, A. K. St. Clair, S. R. Edmondson, and L. T. Taylor, *Inorg. Chem.*, **14**, 478 (1975).

(21) G. N. Schrauzer, *Inorg. Synth.*, 11, 61 (1968).

(22) G. N. Schrauzer and R. J. Windgassen, *J. Am. Chem. Soc.*, **88**, 3738 (1966).

(23) J. B. Raynor, *Inorg. Nucl. Chem. Lett.*, **10**, 867 (1974).

(24) A. H. Maki, N. Edelstein, A. Davison, and R. H. Holm, *J. Am. Chem. Soc.*, **86**, 4580 (1964). The unpaired electron in this system resides on O_2. In terms of the cobalt hyperfine, which arises from spin polarization, we are essentially treating this as a d^7 cobalt system except that a full unpaired electron is not involved, but only fractional spin density from the spin polarization. Since the unpaired electron in these complexes resides on O_2 (vide infra), the *g* tensor is probably determined by the orientation of the coordinated O_2. Co(bzacen)pyO_2 possesses a bent Co–O–O linkage and the EPR spectrum is similar to the other Co–O_2 systems listed in Table I. It is then likely that most (if not all) complexes in Table I possess bent Co–O–O units. As the cobalt hyperfine tensor is likely determined by the surrounding nitrogen and oxygen donor atoms, there is little chance the *g* and cobalt *A* tensors are coincident because of the symmetry of the adduct. The noncoincidence of these two tensors has been shown in a single crystal study of oxycobaltmyoglobin.[26] Though the principal values of the *A* tensor will be larger than those listed in Table I, the reported single-crystal study indicates that frozen solution spectra are a good gauge of the actual anisotropy. The errors introduced in our parameters by these assumptions render them semiquantitative. Under the circumstances, it was not deemed significant to further refine them by incorporating contributions from mixing in quartet states (B. R. McGarvey, *Can. J. Chem.*, **53**, 2498 (1975)). The correction for quartet states is not straightforward in this system for the *g* value observed is associated with the electron on O_2 which even in O_2^- has a value different from that of the free electron. We have made the quartet correction in a series of five- and six-coordinate low spin d^7 complexes and have found it to have only a minor influence on the *A* values and to cause no reversals in trends. The reader is cautioned about these complications in the event he is tempted to use our results for other purposes than the conclusions we draw.

(25) B. R. McGarvey, *J. Phys. Chem.*, 71, 51 (1967).

(26) J. C. W. Chien and L. C. Dickinson, *Proc. Natl. Acad. Sci. U.S.A.*, **69**, 2783 (1972).

(27) T. F. Hunter and M. C. R. Symons, *J. Chem. Soc. A*, 1770 (1967).

(28) M. C. R. Symons, *J. Chem. Soc. A*, 1889 (1970).

(29) P. R. Edwards, S. Subramanian, and M. C. R. Symons, *J. Chem. Soc. A*, 2985 (1968).

(30) M. C. R. Symons and J. G. Wilkinson, *J. Chem. Soc., Faraday Trans. 2*, **68**, 1265 (1972).

(31) A. H. Cohen and B. M. Hoffman, *Inorg. Chem.*, **13**, 1484 (1974).

(32) G. P. Lozos and B. M. Hoffman, *J. Phys. Chem.*, **78**, 200 (1974).

(33) K. M. Wang and J. H. Lunsford, *J. Phys. Chem.*, **73**, 2069 (1969).

(34) W. R. Scheidt, *J. Am. Chem. Soc.*, **96**, 90 (1974).

(35) B. A. Goodman and J. B. Raynor, *Adv. Inorg. Chem. Radiochem.*, **13**, 135 (1970).

(36) B. S. Tovrog and R. S. Drago, to be submitted.

(37) L. F. Mehne and B. B. Wayland, *Inorg. Chem.*, **14**, 881 (1975).

(38) C. J. Weschler, B. M. Hoffman, and F. Basolo, *J. Am. Chem. Soc.*, **97**, 5278 (1975).

(39) W. A. Goddard, III, and B. D. Olafson, *Proc. Natl. Acad. Sci. U.S.A.*, **72**, 2335 (1975).

(40) J. H. Burness, J. G. Dillard, and L. T. Taylor, *J. Am. Chem. Soc.*, **97**, 6080 (1975).

(41) P. Fantucci and V. Valenti, private communication.

(42) Our main conclusion will be shown to be relatively independent of this estimate.

Reversible Oxygen Carriers. The Synthesis and Low Temperature (−171°) Structure of an Unstable Monomeric Dioxygen Adduct of *N,N′*-(1,1,2,2-Tetramethyl)ethylenebis(3-fluorosalicylideniminato)(1-methylimidazole)cobalt(II), Co(3-F-Saltmen)(1-Me-Imid)(O_2)·2(CH_3)$_2$CO

Alex Avdeef and William P. Schaefer*

Contribution No. 5230 from the Arthur Amos Noyes Laboratory of Chemical Physics,
California Institute of Technology, Pasadena, California 91125.
Received December 1, 1975

Abstract: The structure at −171° of *N,N′*-(1,1,2,2-tetramethyl)ethylenebis(3-fluorosalicylideniminato)(1-methylimidazole)superoxocobalt(III) diacetone solvate, Co(3-F-Saltmen)(1-Me-Imid)(O_2)·2(CH_3)$_2$CO, has been determined from three-dimensional x-ray data collected by counter methods and has been refined on F^2 using 6078 reflections, including those with negative intensities. The conventional R_F factor based on the portion of the data with F^2 greater than $3\sigma(F^2)$ is 6.0%. The monomeric adduct (Co:O_2 = 1:1) of cobalt(II) crystallizes in the monoclinic space group $C^5{}_{2h}$-$P2_1/c$ (No. 14), with four formula units in a cell with the low-temperature dimensions a = 11.934 (6) Å, b = 13.864 (5) Å, c = 18.018 (8) Å, and β = 92.35 (2)°. The superoxide ligand, O_2^-, is bonded "end-on" to the cobalt atom of the chelate, with a Co–O–O angle of 117.4 (2)° and an O–O bond length of 1.302 (3) Å. The dioxygen group lies nearly in the plane defined by the methylimidazole trans to it. The Co–O (dioxygen) and Co–N (imidazole) bond distances are 1.881 (2) and 2.004 (3) Å, respectively. The other coordination bonds average 1.893 (Co–N) and 1.901 Å (Co–O). The molecular packing in the vicinity of the coordinated dioxygen ligand is similar to that found in the hydrophobic "distal imidazole" pocket of myoglobin. Crystals of the cobalt oxygen adduct are not stable at ambient conditions and evolution of O_2 may be readily observed, as the crystals change from dark burgundy red to golden yellow upon decomposition.

Understanding molecular oxygen transport and storage in living systems has been enhanced by studies of reversibly bound dioxygen adducts of simple transition metal complexes.[1] Much effort has been directed towards the mimicry of myoglobin and hemoglobin, as demonstrated so well by the characterization of the dioxygen adduct of the iron "picket fence porphyrin" complex by Collman and co-workers.[2]

Schiff base complexes of cobalt(II) have been studied as oxygen carriers since 1938.[3] The relevance and importance of such dioxygen-carrying cobalt complexes as models has been elegantly demonstrated by Hoffman[4] and others.[5] Of particular interest are the "end-on" bonded monomeric ($Co:O_2$ = 1:1) species. However, the isolation of such species has been difficult due to their fragile stability at ambient conditions and the facile formation of the thermodynamically more stable 2:1 adducts,

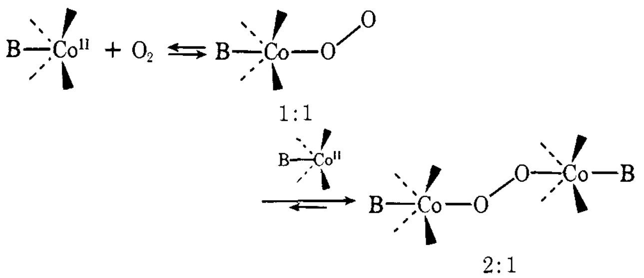

The latter dimerization step can be minimized by working at low temperatures, using dilute solutions, avoiding sources of hydrogen bonding,[6] utilizing steric hindrance,[2,7] and by choosing an appropriate axial base, B.[8] Only recently has the structural basis for the reversibility in dioxygen coordination been illuminated by the reports of several structures of 1:1 complexes.[2,9–13] Unfortunately the accuracy and reliability of some of the results have been compromised by the presence of varying degrees of disorder.

Some of our own recent efforts have been to synthesize stable 1:1 adducts with *N,N'*-(1,1,2,2-tetramethyl)ethylenebis(3-R-salicylideniminato)(1-R'-imidazole)cobalt(II), Co(3-R-Saltmen)(1-R'-Imid), where R and R' are substituent groups

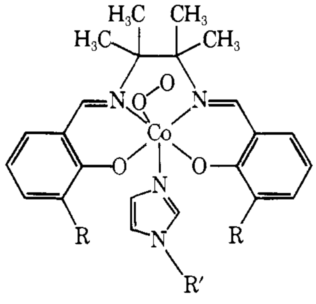

1, R = *t*-Bu; R' = benzyl
2, R = H; R' = benzyl
3, R = F; R' = CH_3

of varying steric and electronic character. The crystal structure of one such dioxygen adduct with R = *tert*-butyl and R' = benzyl, **1**, has already been reported,[12] with diffraction data collected both at 19° and −154°. The room temperature structure of the exceptionally stable 1:1 species with R = H and R' = benzyl, **2**, has just been completed.[13] Cobalt complexes with R = NO_2, CF_3, and MeO are being currently examined. The subject of the present report is the synthesis and the low temperature (−171°) structure of a moderately unstable monomeric dioxygen adduct with R = F and R' = methyl, [Co(3-F-Saltmen)(1-Me-Imid)(O_2)]·2$(CH_3)_2CO$, **3**.

Experimental Section

The purchased chemicals were used without further purification. Analyses were performed by the analytical laboratory at Caltech.

Preparation of *N,N'*-(1,1,2,2-Tetramethyl)ethylenebis(3-fluorosalicylidenimine), 3-F-Saltmen H_2. 2,3-Diamino-2,3-dimethylbutane (1.2 ml, ~10 mmol) (prepared by the reduction of the dinitro compound[14]) was slowly added to 2.8 g (~20 mmol) of 3-fluorosalicylaldehyde (Marshallton Research Laboratories, Inc.) dissolved in 30 ml of boiling 95% ethanol. Upon cooling to room temperature, brilliant yellow crystal flakes precipitated. The Schiff base was collected and dried in vacuo for 12 h at 100°. Yield 2.5 g (70%). Anal. Calcd ($C_{20}H_{22}N_2O_2F_2$): C, 66.7; H, 6.2; N, 7.8. Found: C, 65.8; H, 6.1; N, 7.6.

Table I. Crystal Data for [Co(3-F-Saltmen)(1-Me-Imid)(O_2)]·2acetone

Molecular formula: $C_{30}H_{38}CoF_2O_6N_4$; FW = 647.6 g
d_{calcd} = 1.444 (1)[a] g cm^{-3}; Formula units/cell = 4
Linear absorption coefficient, μ = 6.7 cm^{-1} (Mo Kα radiation)
Crystal dimensions: A slightly irregularly shaped platelet, bounded primarily by {100}, {011}, and {01$\bar{1}$} faces with the respective approximate thicknesses: 0.18, 0.65, and 0.53 mm
Systematic absences: $h0l$, $l = 2n + 1$; $0k0$, $k = 2n + 1$
Space group: C^5_{2h}-$P2_1/c$ (No. 14)
Cell parameters:
297 ± 1 K: a = 12.06, b = 13.96, c = 18.41 Å; β = 91.5° (photographically determined, using two crystals)
102 ± 3 K: a = 11.934 (6), b = 13.864 (5), c = 18.018 (8) Å; β = 92.35 (2)° (mean values of several different orientations on the diffractometer, using graphite-monochromatized Mo Kα radiation, λ 0.710688 Å)

$$\text{Cell volume: } U = \begin{cases} 3096\ \text{Å}^3\ (297\ \text{K}) \\ 2979\ (2)\ \text{Å}^3\ (102\ \text{K}) \end{cases}$$

F_{000} = 1356 e

[a] The value in parentheses following a quantity here and elsewhere in the report refers to the estimated standard deviation (esd) in the least significant digit.

Preparation of *N,N'*-(1,1,2,2-Tetramethyl)ethylenebis(3-fluorosalicylideniminato)cobalt(II), Co(3-F-Saltmen). Under nitrogen, 1.25 g (5 mmol) of cobalt acetate, $Co(OAc)_2·4H_2O$, dissolved in 20 ml of boiling hot water, was added slowly to a briskly stirred slurry of 1.80 g (5 mmol) of 3-F-Saltmen H_2 and 2.26 g (10 mmol) of $NaOAc·3H_2O$ in 30 ml of refluxing 95% ethanol. The solution was stirred 5 min further and allowed to cool; small bright red crystals precipitated. The solid was filtered, washed several times with cold water, and dried in vacuo over P_2O_5 for 24 h at 100°. Yield 1.96 g (90%). Anal. Calcd ($C_{20}H_{20}N_2O_2F_2Co$): C, 57.6; H, 4.8; N, 6.7. Found: C, 57.6; H, 5.0; N, 6.8.

Preparation of *N,N'*-(1,1,2,2-Tetramethyl)ethylenebis(3-fluorosalicylideniminato)(1-methylimidazole)superoxocobalt(III) Diacetonate, Co(3-F-Saltmen)(1-Me-Imid)(O_2)·2$(CH_3)_2CO$. A 25 ml volumetric flask was suspended in a cold bath maintained at −18° and 15 ml of spectroscopic grade acetone was placed in it; then 0.082 g (0.19 mmol) of Co(3-F-Saltmen) was added followed by one drop of 1-methylimidazole (approximately an equivalent). Thoroughly dried oxygen gas was passed over the surface of the solution and it quickly turned dark. After 10–24 h large, heavily intergrown, dark burgundy red crystals formed. Attempts were made to grow crystals from acetonitrile, tetrahydrofuran, and dichloromethane solutions, but none of these solvents produced crystals.

Crystal Handling and Diffraction Data Collection. Most attempts to mount crystals on glass fibers with any of the fixatives available to us proved unsuccessful because the complex decomposed almost immediately with the evolution of oxygen bubbles through the fixative layer. Most often crystals began to change from dark red to golden yellow within 5 min of exposure to just the ambient conditions of the laboratory. However, on two occasions, epoxy-mounted crystals unexpectedly remained stable for several hours, long enough for film inspection at room temperature. Generally the crystals remained indefinitely stable when stored in the freezer compartment (−15°) of our refrigerator. On one occasion a sample inadvertantly left for 1 week in the warmer compartment (5°) of the refrigerator decomposed to a bright red rather than the usual yellow material.

In view of the thermal instability, we decided to collect intensity data at low temperature. A four-circle Picker FACS-I automatic diffractometer, utilizing graphite monochromatized Mo Kα radiation (λ 0.71069 Å) and equipped with an Enraf Nonius Delft low-temperature device, was used. The temperature was maintained for 5 weeks at −171 ± 3°. The crystals examined on the diffractometer were quickly mounted at room temperature on the broken ends of thin quartz capillaries, using silicone grease, and were immediately placed into the cold nitrogen stream. Unfortunately, it was not possible to assess crystal quality by film methods prior to diffractometer exam-

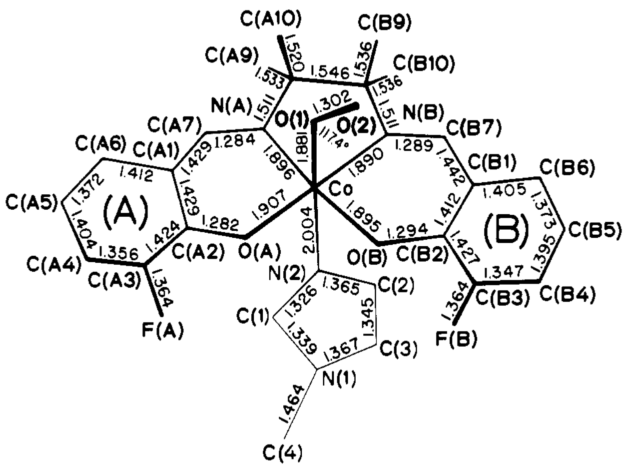

Figure 1. Bond distances and labeling scheme for the dioxygen adduct. The estimated standard deviations in the bond lengths are: σ(Co–O), σ(Co–N), and σ(O–O) ~0.002–0.003 Å; σ(C–O) and σ(C–N) ~0.004–0.005 Å; σ(C–C) ~0.005–0.006 Å.

ination. The crystal chosen for data collection had acceptable ω scan widths at half heights of 0.09–0.15° for about a dozen strong reflections, using a 3.5° tube takeoff angle. The crystal was relatively large, and originally had a smaller crystal plate growing out of one of its faces. Upon the delicate removal of the intrusion, a shallow pit remained, possibly lined with a small amount of amorphous material. The various crystal data are summarized in Table I.

Over 11 000 reflections were measured by the moving crystal, moving counter scan technique at a rate of 2° min^{-1} out to $2\theta_{\max} = 53°$, using a takeoff angle of 3.5°, and employing 20-s stationary background counts at the limits of each scan. In addition to one complete quadrant, data were collected in all quadrants in the 2θ intervals 0–20, 28–30, and 49–50°, thus affording us some 3000 duplicates for assessing the quality of our data. The intensities of three reflections were monitored approximately once an hour initially, and at longer intervals when crystal and diffractometer stability became apparent.

The intensities were corrected for the usual Lorentz and polarization effects. No absorption corrections were applied. The reduced intensities and the associated errors are defined elsewhere.[15] The Peterson-Levy error factor,[16] p, was first assumed to be 4%. There were 6078 unique reflections collected, of which 3889 had $F^2/\sigma(F^2) > 3$ and 5500 had $F^2 > 0$.

Error Analysis. The duplicate reflections from four symmetry-equivalent forms were used to obtain the experimental value of p = 5.6% by a self-consistency method.[17] The results of the evaluation are presented in Table II. The errors, although somewhat large, are not systematically distributed as a function of ϕ and χ diffractometer settings.[17] The intensity dependence is essentially accounted for by the experimental p factor.

Solution and Refinement of the Structure. Direct methods were employed to solve the structure, using MULTAN 74.[19] About 90% of the structure was produced in the lineprinter plot of the program-recognized molecular fragments. The remaining atoms were generated using reasonable estimates of the bond lengths and angles associated with the missing atoms.

A difference electron density map[20] clearly indicated the presence of the hydrogen atoms and two independent molecules of acetone. Using the 3σ reflections ($F^2/\sigma(F^2) \geq 3$) 11 cycles of blocked-matrix least-squares refinement[22] led to an essentially converged model. Two additional cycles were performed, where all of the 6078 reflections, including those with negative intensities,[24] were used and where the hydrogen atom parameters were allowed to vary.[25]

The final difference map had one peak of height 1.0 e/Å^3, located near the cobalt and the imidazole nitrogen atoms, with no obvious interpretation. All other residual peaks were below +0.5 and above −0.5 e/Å^3. The final standard R_F factor for the 3σ data was 6.0%, and for the data with $F^2 > 0$, it was 8.7%. $R_{wF}(3\sigma)$ = 7.4% and GOF[22] (all data) = 1.80. Agreement analysis[17] of the observed and calculated structure factors confirmed that the experimental p factor was properly chosen.[26] The final parameters are presented in Table III.

Results and Discussion

The calculated bond distances are presented in Figure 1. Figure 2 shows the thermal ellipsoid representation of the monomeric adduct and the two acetone molecules which embrace the dioxygen ligand.

Table II. Error Analysis Using Symmetry-Equivalent Reflections[a]

Quadrant	R_{F^2}	R_{wF^2}	GOF	No. of refl	Slope[b]	Intercept[b]
$\pm h, k, l$	0.053	0.074	1.40	695	1.13	−0.49
$\pm h, k, \bar{l}$	0.047	0.066	1.11	693	1.04	+0.24
$\pm h, \bar{k}, l$	0.039	0.068	1.08	682	1.00	+0.26
$\pm h, \bar{k}, \bar{l}$	0.062	0.097	1.41	641	1.26	+0.05
Mean	0.047	0.075	1.12			

[a] R_{F^2}, R_{wF^2}, and GOF (goodness-of-fit) are agreement factors based on deviations from the means of sets of duplicate reflections.[17] On the last cycle, p (input) = 0.054 and p (output) = 0.058. The value 0.056 was used in calculating the final σ. [b] Slope and intercept refer to Abrahams-Keve[18] type of normal probability plots. The expected values are unity and zero, respectively.

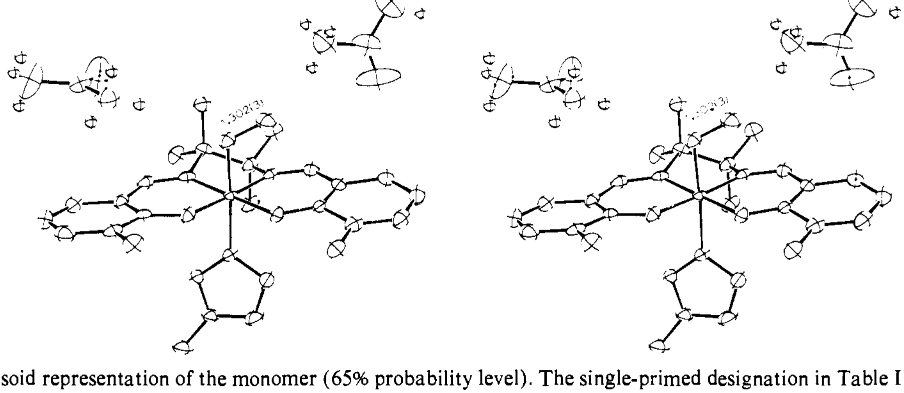

Figure 2. Thermal ellipsoid representation of the monomer (65% probability level). The single-primed designation in Table III applies to the acetone molecule on the left, while the double-primed molecule is on the right.

Table III. Atomic Parameters[a]

	x	y	z	U_{11}	U_{22}	U_{33}	U_{12}	U_{13}	U_{23}	Rms amplitudes (Å)		
										1	2	3
Co	−689 (0.4)	6109 (0.4)	2090 (0.3)	16 (0.3)	10 (0.3)	10 (0.3)	0 (0.2)	−1 (0.2)	0 (0.2)	0.095	0.101	0.127
O (1)	−320 (2)	7099 (2)	2771 (2)	20 (2)	16 (2)	21 (2)	−2 (1)	−3 (1)	−1 (1)	0.122	0.133	0.156
O (2)	−1057 (2)	7779 (2)	2851 (2)	32 (2)	19 (2)	25 (2)	1 (1)	−1 (1)	−7 (1)	0.098	0.119	0.147
N(A)	−134 (3)	5191 (2)	2794 (2)	21 (2)	13 (2)	13 (2)	−3 (1)	0 (1)	−2 (1)	0.106	0.143	0.152
O(A)	726 (2)	6392 (2)	1687 (1)	18 (2)	20 (2)	17 (1)	4 (1)	−2 (1)	4 (1)	0.096	0.105	0.157
C(A1)	1782 (3)	5194 (3)	2392 (2)	19 (2)	14 (2)	17 (2)	1 (2)	−4 (2)	−2 (2)	0.118	0.134	0.139
C(A2)	1650 (3)	5964 (3)	1868 (2)	16 (2)	16 (2)	14 (2)	0 (2)	−1 (2)	−5 (2)	0.108	0.128	0.144
C(A3)	2662 (3)	6254 (3)	1540 (2)	24 (2)	13 (2)	15 (2)	−3 (2)	−2 (2)	−1 (2)	0.119	0.168	0.182
C(A4)	3677 (4)	5834 (3)	1671 (2)	23 (2)	25 (2)	24 (2)	−5 (2)	4 (2)	−8 (2)	0.110	0.120	0.154
C(A5)	3784 (4)	5071 (3)	2182 (2)	17 (2)	29 (2)	25 (2)	5 (2)	−3 (2)	0 (2)	0.097	0.127	0.143
C(A6)	2844 (4)	4766 (3)	2528 (2)	24 (2)	19 (2)	21 (2)	−0 (2)	−4 (2)	−0 (2)	0.105	0.124	0.159
C(A7)	881 (3)	4883 (3)	2833 (2)	26 (2)	14 (2)	14 (2)	3 (2)	−4 (2)	1 (2)	0.129	0.144	0.186
C(A8)	−929 (3)	4916 (3)	3390 (2)	23 (2)	15 (2)	14 (2)	0 (2)	4 (2)	4 (2)	0.119	0.160	0.173
C(A9)	−701 (4)	3891 (3)	3678 (2)	28 (2)	22 (2)	23 (2)	−1 (2)	−2 (2)	9 (2)	0.129	0.138	0.167
C(A10)	−738 (4)	5621 (3)	4029 (2)	22 (2)	29 (3)	17 (2)	−0 (2)	0 (2)	−3 (2)	0.106	0.121	0.169
F(A)	2583 (2)	7012 (2)	1059 (1)	27 (1)	22 (1)	24 (1)	−2 (1)	2 (1)	5 (1)	0.102	0.131	0.152
N(B)	−2079 (3)	5874 (2)	2524 (2)	22 (2)	11 (2)	12 (2)	−0 (1)	−4 (1)	−1 (1)	0.118	0.161	0.181
O(B)	−1248 (2)	7030 (2)	1392 (1)	19 (2)	18 (2)	15 (1)	2 (1)	−1 (1)	1 (1)	0.124	0.151	0.173
C(B1)	−3123 (3)	7131 (3)	1851 (2)	22 (2)	10 (2)	18 (2)	3 (2)	−5 (2)	−4 (2)	0.131	0.161	0.170
C(B2)	−2254 (3)	7381 (3)	1379 (2)	20 (2)	14 (2)	12 (2)	2 (2)	−5 (2)	−1 (2)	0.089	0.119	0.168
C(B3)	−2568 (3)	8064 (3)	815 (2)	25 (2)	15 (2)	17 (2)	−1 (2)	−2 (2)	1 (2)	0.097	0.115	0.151
C(B4)	−3597 (4)	8459 (3)	731 (2)	31 (3)	14 (2)	24 (2)	2 (2)	−8 (2)	1 (2)	0.122	0.124	0.164
C(B5)	−4431 (4)	8216 (3)	1218 (3)	20 (2)	22 (2)	32 (3)	4 (2)	−5 (2)	0 (2)	0.115	0.133	0.195
C(B6)	−4184 (3)	7569 (3)	1778 (2)	20 (2)	16 (2)	27 (2)	1 (2)	−3 (2)	−4 (2)	0.124	0.153	0.189
C(B7)	−2975 (3)	6379 (3)	2400 (2)	18 (2)	15 (2)	21 (2)	0 (2)	−3 (2)	−1 (2)	0.123	0.134	0.173
C(B8)	−2121 (3)	5004 (3)	3028 (2)	23 (2)	19 (2)	18 (2)	0 (2)	−2 (2)	3 (2)	0.122	0.129	0.150
C(B9)	−2999 (4)	5119 (4)	3621 (3)	26 (2)	27 (2)	24 (2)	0 (2)	6 (2)	8 (2)	0.122	0.143	0.154
C(B10)	−2440 (4)	4128 (3)	2543 (3)	30 (2)	18 (2)	25 (2)	−6 (2)	−6 (2)	1 (2)	0.123	0.162	0.187
F(B)	−1758 (2)	8307 (2)	337 (1)	29 (1)	24 (1)	19 (1)	4 (1)	2 (1)	7 (1)	0.122	0.142	0.195
N(1)	−725 (3)	3905 (2)	525 (2)	31 (2)	16 (2)	17 (2)	8 (2)	−2 (2)	−5 (2)	0.119	0.159	0.181
N(2)	−950 (3)	5112 (2)	1296 (2)	19 (2)	16 (2)	14 (2)	−1 (2)	−2 (1)	−1 (2)	0.102	0.135	0.188
C(1)	−322 (3)	4356 (3)	1137 (2)	21 (2)	18 (2)	5 (2)	3 (2)	−2 (2)	−1 (2)	0.118	0.129	0.153
C(2)	−1796 (4)	5131 (3)	763 (3)	31 (3)	28 (3)	30 (3)	11 (2)	−15 (2)	−8 (2)	0.121	0.145	0.234
C(3)	−1669 (4)	4394 (3)	289 (3)	45 (3)	30 (3)	26 (3)	10 (2)	−19 (2)	−16 (2)	0.097	0.159	0.258
C(4)	−230 (4)	3057 (3)	182 (3)	42 (3)	22 (2)	19 (2)	7 (2)	2 (2)	−7 (2)	0.110	0.161	0.209
O(′)	2135 (3)	5838 (3)	4535 (2)	40 (2)	105 (4)	66 (3)	1 (2)	4 (2)	52 (3)	0.169	0.202	0.374
C(1′)	2530 (4)	7017 (4)	3648 (3)	38 (3)	28 (3)	31 (3)	5 (2)	−5 (2)	3 (2)	0.150	0.180	0.202
C(2′)	2839 (4)	6274 (3)	4222 (2)	32 (3)	29 (3)	19 (2)	−3 (2)	−2 (2)	−1 (2)	0.136	0.165	0.182
C(3′)	4032 (5)	6077 (5)	4377 (4)	44 (4)	46 (4)	78 (5)	−9 (3)	−22 (3)	22 (4)	0.182	0.193	0.314
O(″)	−4571 (4)	7768 (3)	3589 (2)	98 (3)	86 (3)	42 (2)	−53 (3)	17 (2)	−12 (2)	0.191	0.198	0.383
C(1″)	−2842 (6)	8297 (5)	4082 (3)	63 (4)	47 (4)	39 (3)	20 (3)	13 (3)	11 (3)	0.173	0.188	0.287
C(2″)	−4071 (5)	8255 (4)	4046 (3)	60 (4)	30 (3)	31 (3)	−10 (3)	14 (3)	6 (2)	0.133	0.192	0.256
C(3″)	−4669 (5)	8804 (4)	4628 (4)	52 (4)	45 (4)	67 (4)	3 (3)	19 (3)	−4 (3)	0.197	0.212	0.280

	x	y	z	B (Å^2)		x	y	z	B (Å^2)
H(1)	438 (3)	609 (3)	145 (2)	2.3 (9)	H(20)	−283 (4)	465 (3)	396 (2)	3.8 (10)
H(2)	444 (3)	469 (3)	227 (2)	1.2 (10)	H(21)	−188 (3)	401 (3)	220 (2)	2.4 (9)
H(3)	284 (3)	420 (3)	287 (2)	2.4 (9)	H(22)	−312 (3)	424 (3)	231 (2)	4.2 (9)
H(4)	114 (3)	445 (3)	319 (2)	1.7 (9)	H(23)	−256 (3)	358 (3)	285 (2)	2.1 (10)
H(5)	−375 (3)	888 (3)	41 (2)	1.9 (9)	H(24)	3 (3)	323 (3)	−31 (2)	2.9 (9)
H(6)	−518 (3)	854 (3)	118 (2)	1.8 (9)	H(25)	−72 (3)	259 (3)	12 (2)	3.5 (9)
H(7)	−474 (3)	744 (3)	215 (2)	1.6 (9)	H(26)	40 (4)	283 (3)	49 (2)	3.1 (10)
H(8)	−371 (3)	623 (3)	265 (2)	2.0 (9)	H(27)	267 (3)	769 (3)	385 (2)	3.3 (9)
H(9)	27 (3)	414 (3)	144 (2)	2.2 (9)	H(28)	169 (4)	709 (3)	355 (2)	3.3 (10)
H(10)	−239 (3)	560 (3)	81 (2)	1.2 (10)	H(29)	295 (4)	693 (3)	325 (3)	3.9 (10)
H(11)	−209 (4)	421 (3)	−13 (2)	2.3 (10)	H(30)	421 (4)	560 (4)	476 (3)	3.4 (12)
H(12)	−65 (3)	341 (3)	327 (2)	1.7 (9)	H(31)	426 (5)	570 (4)	400 (3)	6.1 (12)
H(13)	−140 (3)	357 (3)	395 (2)	1.2 (9)	H(32)	439 (4)	658 (4)	456 (3)	5.4 (12)
H(14)	−3 (3)	387 (3)	398 (2)	3.1 (9)	H(33)	−259 (4)	895 (4)	402 (3)	5.2 (12)
H(15)	−110 (3)	632 (3)	391 (2)	0.9 (9)	H(34)	−256 (4)	811 (4)	455 (3)	5.6 (12)
H(16)	−118 (3)	549 (3)	440 (2)	1.7 (9)	H(35)	−261 (5)	785 (4)	380 (3)	5.9 (13)
H(17)	5 (3)	565 (3)	420 (2)	3.5 (9)	H(36)	−443 (4)	944 (4)	461 (3)	6.0 (12)
H(18)	−375 (3)	503 (3)	344 (2)	1.1 (9)	H(37)	−552 (4)	873 (3)	447 (3)	5.1 (12)
H(19)	−292 (3)	580 (3)	387 (2)	1.7 (10)	H(38)	−457 (4)	849 (4)	510 (3)	6.8 (13)

[a] The x, y, z fractional coordinates are multiplied by 10^4 in the case of non-hydrogen atoms and by 10^3 otherwise. The form of the thermal ellipsoid is $\exp[-2\pi^2(U_{11}h^2a^{*2} + \ldots + 2U_{23}klb^*c^*)]$. The U_{ij} elements in the table are multiplied by 10^3.

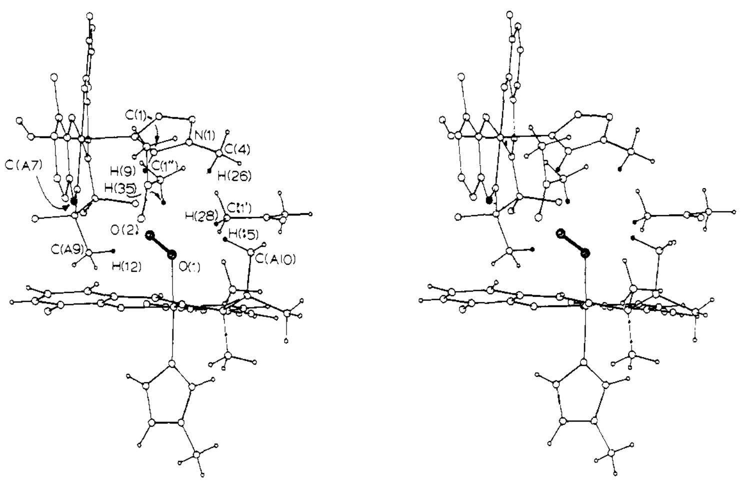

Figure 3. A detailed view of the packing in the vicinity of the coordinated O_2. The various distances of interest are presented in Table IV. Note the general similarity to the "distal imidazole" pocket in myoglobin (cf. Figure 4).

The O(1)-O(2) bond length in **3**, 1.302 (3) Å, is slightly longer than the values reported for other 1:1 species,[2,9-13] but is in reasonable accord with the expected value of 1.28 Å[28] for the superoxide (O_2^-) ligand. The corresponding value in **1** is 1.273 (10) at −154° and 1.257 (10) Å at 19°, while in **2** it is 1.277 (3) Å. Since substituent groups on the benzene ring can markedly affect the electronic structure of the metal in Co-Salen compounds (Salen = *N,N'*-ethylenebis(salicylidenimine)), as shown by the infrared study of nitrosyl adducts,[29] where shifts in ν(N-O) can be as high as 70 cm^{-1}, it is surprising that the dioxygen bond length in **3** is *longer* than found in **1** or **2**, since the fluorine atoms are expected to withdraw electron density from the cobalt atoms, thus leading to *reduced* antibonding valence electron population in the O_2^- species. We are at a loss to explain the observed trend. The differences between the three structures are probably significant, but any conclusions must await larger sampling.

Bond angles in the complex are quite normal for salicylaldehyde complexes. The two N-Co-O in-plane angles are 95.7 and 95.9°; N-Co-N is 84.1° and O-Co-O is 84.3°. The oxygen atom of the O_2 group bonded to Co is not on a line through the Co atom and normal to the ligand plane; the angle between the normal and the Co-O(1) vector is 3.8°. This is smaller than the 5.3° found by Brown and Raymond[11] for $(CN)_5CoO_2^{3-}$, but the displacement in the two structures is in the same direction.

By polarizing the filled, out-of-plane, metal t_{2g} d orbitals, the π-donor imidazole ligand is expected to reinforce the back-bonding of electron density into the empty π^* orbital of the dioxygen ligand in the trans position when the latter lies in the imidazole-defined plane. Structural evidence for such an effect has been scarce. In the "picket fence" adduct, only one of the two disordered dioxygen molecules lies in the plane, suggesting the effect to be of minimal importance in that case. It seems likely that in myoglobin, the O_2 ligand also lies somewhat out of the plane (vide infra). In the present compound, **3**, as in **1** and **2**, the axial methyl groups on the ethylenediamine bridge rigidly constrain the imidazole ligand plane to bisect the *N*(imine)-Co-O(phenolic) angle, an orientation which leads to stronger Co-N(imidazole) bonds due to decreased steric hindrance between the base and the Schiff base plane.[30] On the other hand, the O_2 molecule can rotate about its coordination axis over a range of 180°. Yet in structures **1-3** the dioxygen species essentially lies in the imidazole plane, perhaps suggesting the presence of some stabilization arising from enhanced π^* back-bonding in the O_2 ligand. The dihedral angle between the average imidazole plane and the plane formed by Co-O(1)-O(2) is 12.6° in **3** and 18.5° in **1**.

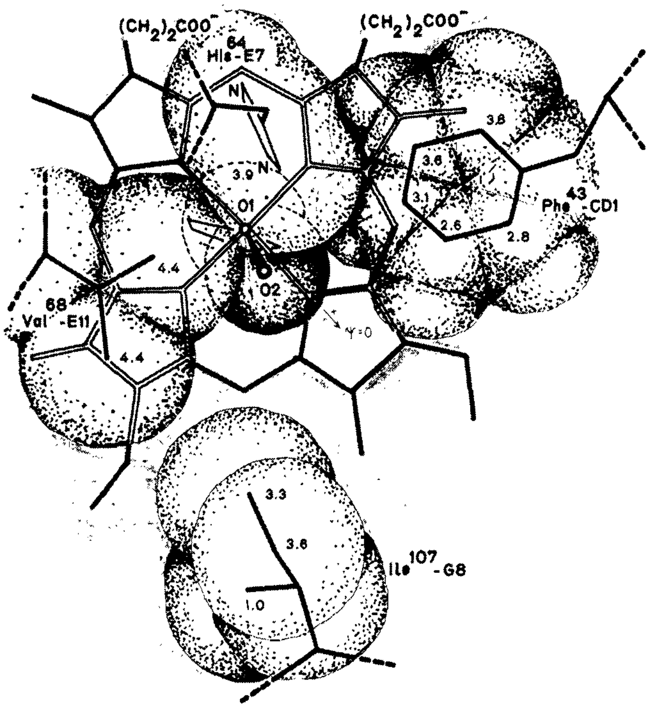

Figure 4. The view of the "distal imidazole" hydrophobic pocket in metmyoglobin using Watson's[31] 1.4 Å resolution coordinates. The shaded groups (van der Waals radii) above the porphyrin plane are interlocked to form a unique cavity for the oxygen molecule, shown here in the hypothetical minimum-repulsion orientation (see text). The distal imidazole is labeled His^{64}-E7. The numbers adjacent to the shaded atoms are the distances, in Å, above the mean porphyrin plane.

Figure 3 focuses on the molecular packing in the vicinity of the dioxygen ligand and Table IV lists some of the distances and angles of interest. The dioxygen molecule is snuggly embraced by aprotic groups on all sides. The two molecules of acetone play an integral part in "locking" the dioxygen atoms in one orientation. They are not held strongly, however, and the acetone can escape from the crystal by diffusing out passage ways parallel to the *c* axis; when this happens the crystal disintegrates completely.

The environment of the dioxygen ligand in **3** (as well as **1**) is remarkably similar to the hydrophobic, oxygen-coordinating pocket of myoglobin.[31] In **3**, the imidazole from a neighboring molecule is very close to the dioxygen ligand, as in the natural system. Both cases have the dioxygen ligand also surrounded by methyl groups. Figure 4 shows the "distal imidazole" side

Table IV. Selected Nonbonded Contact Distances (in Å) and Angles (in deg)[a]

Contact	Distance	Contact	Distance	Contact	Distance
Non-Hydrogen Contacts under 3.4 Å					
O(2)···C(A10)	3.110 (5)	F(B)···C(A10)^{II}	3.079 (7)	F(A)···C(3)^{III}	3.266 (7)
···C(A7)^{I}	3.176 (7)	···C(4)^{III}	3.202 (7)	C(A5)···C(2″)^{V}	3.379 (8)
···C(1)^{I}	3.251 (7)	···C(1″)^{IV}	3.390 (8)		
Hydrogen Contacts[b]					
O(2)···H(9)^{I}	2.44 (5)	F(A)···H(11)^{III}	2.44 (5)		
···H(35)	2.57 (5)	···H(13)^{I}	2.59 (5)		
···H(15)	2.79 (4)	F(B)···H(16)^{IV}	2.49 (5)		
···H(12)^{I}	3.05 (5)	···H(14)^{I}	2.54 (5)		
···H(26)^{I}	3.06 (5)	···H(34)^{IV}	2.58 (6)		
O(1)···H(15)	2.53 (4)	O(A)···H(24)^{III}	2.66 (5)		
···H(28)	2.73 (5)	O(B)···H(24)^{III}	2.51 (5)		
···H(12)^{I}	2.89 (5)				
Angles					
C(1)^{I}-H(9)^{I}···O(2)	147 (3)	H(35)···O(2)-O(1)	128 (1)		
C(1″)-H(35)···O(2)	134 (5)	H(15)···O(1)-O(2)	87 (1)		
H(9)^{I}···O(2)-O(1)	112 (1)				

[a] Roman numeral superscripts refer to equivalent positions relative to the reference molecule at x, y, z: I = $(\bar{x}, y + 1/2, 1/2 - z)$, II = $(x - 1, 3/2 - y, 1/2 + z)$, III = $(\bar{x}, 1 - y, \bar{z})$, IV = $(x - 1, 3/2 - y, z - 1/2)$, and V = $(\bar{x}, y - 1/2, 1/2 - z)$. The hydrogen labeling scheme is partly identified in Figure 3 and completely in Table VII.[35] [b] The calculated esd's given here should probably be at least doubled to take into account the fact that the C-H distances do not represent true internuclear distances.

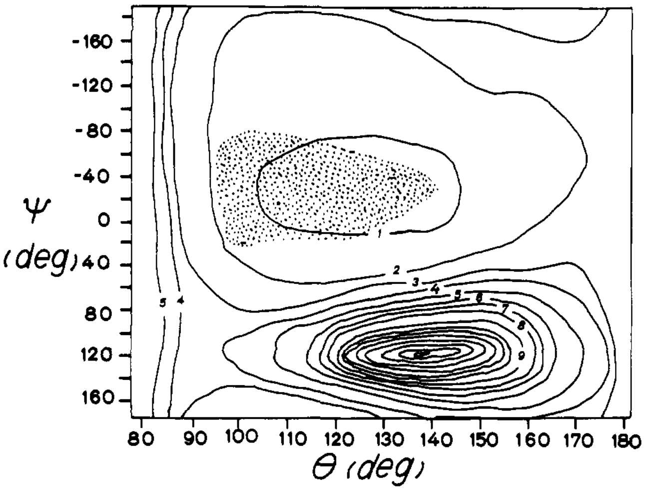

Figure 5. Contoured plot of $\sum 1/r^6$ (relative arbitrary units) as a function of θ(Fe-O-O) angle and ψ(N_{pyr}-Fe-O-O) torsion angle. The contact distances, r, are between the terminal oxygen and the various adjacent groups. $\psi = 0$ is defined in Figure 4. The shaded area represents the region where only reasonable contact distances are found.

of the porphyrin plane, with the dioxygen ligand placed into a "minimum repulsion" region based on a simple electrostatic model. For various values of the Fe-O-O angle, θ, and the torsion angle N(pyrrole)-Fe-O-O, ψ, the sum of the $1/r^6$ terms of the four closest contacts to the uncoordinated oxygen is shown in Figure 5; a shallow minimum is observed. On this basis we estimate that the Fe-O-O angle is about 120 ± 10° and the torsion angle ψ about −30 ± 10° (cf. Figure 4). This orientation of the dioxygen ligand is supported by the single-crystal electron spin resonance study of cobalt-reconstituted myoglobin.[5] However, the latter study predicts a symmetrical π bonding for the O_2 ligand, a view not supported by recent accurate structural results of 1:1 adducts and the simple repulsion model for the hydrophobic pocket.

The dimensions of the Salen portion in the present structure agree well with those of **1** and **2** and with the majority of other six-coordinate Salen-containing structures,[32] with the exception of the phenolic C-O bond distances, which in the present case (1.288 Å average) seem to be shorter than previously observed. This is in accord with the expected effect of the fluorine atoms in making the phenolic atoms more acidic.

The methylimidazole dimensions agree well with the most accurate previous determinations.[33] The imidazole atoms rigorously lie in a plane (Table V). Rigid-body libration-translation analysis[34] reveals a 6.3° root-mean-square (rms) rotation (negligible pitch) of the imidazole group approximately about the coordination bond. Similar analysis shows that the acetone molecules librate in a complicated manner with rms amplitudes as high as 9-12°.

Acknowledgment. We wish to thank Professor K. N. Raymond and his associates, E. C. Baker, F. R. Fronczek, and G. W. Halstead, for allowing us the use of their laboratory and diffractometer and for providing us with indispensable assistance. We wish to thank R. E. Marsh for his continued interest in our work and for several illuminating discussions on the subject of this paper. This work was supported in part by the National Heart and Lung Institute under Grant No. HL-12395; we are grateful for this assistance.

Supplementary Material Available. Table V, Table VI, containing calculated bond angles, Table VII, containing the complete hydrogen atom labeling scheme along with the C-H distances, and Table VIII, listing the observed and calculated structure-factor amplitudes (27 pages). Ordering information is given on any current masthead page.

References and Notes

(1) (a) M. N. Hughes, "The Inorganic Chemistry of Biological Processes", Wiley, New York, N.Y., 1972, Chapter 7; (b) J. M. Rifkind in "Inorganic Biochemistry", G. L. Eichhorn, Ed., Elsevier, Amsterdam, 1973, Chapter 25; (c) J. S. Valentine, *Chem. Rev.*, **73**, 235 (1973); (d) G. Henrici-Olive and S. Olive, *Angew. Chem., Int. Ed. Engl.*, **13**, 29 (1974).
(2) J. P. Collman, R. R. Gagne, C. A. Reed, W. T. Robinson, and G. A. Rodley, *Proc. Natl. Acad. Sci. U.S.A.*, 71, 1326 (1974).
(3) T. Tsumaki, *Bull. Chem. Soc. Jpn.*, **13**, 252 (1938); (b) E. W. Hughes, W. K. Wilmarth, and M. Calvin, *J. Am. Chem. Soc.*, **68**, 2273 (1946), and references therein.
(4) B. M. Hoffman and D. H. Petering, *Proc. Natl. Acad. Sci. U.S.A.*, **67**, 637 (1970).
(5) J. C. W. Chien and L. C. Dickinson, *Proc. Natl. Acad. Sci. U.S.A.*, **69**, 2783 (1972).
(6) D. V. Stynes, H. C. Stynes, J. A. Ibers, and B. R. James, *J. Am. Chem. Soc.*, **95**, 1142 (1973).
(7) (a) G. G. Christoph, J. F. Rogers, and W. P. Schaefer, American Crystallographic Association, Winter Meeting, Gainesville, Fla., Jan 1973, Paper D1; (b) J. E. Baldwin and J. Huff, *J. Am. Chem. Soc.*, **95**, 5758 (1973); (c) J. Almog, J. E. Baldwin, and J. Huff, *ibid.*, **97**, 227 (1975); (d) M. Calligaris, G. Nardin, and L. Randaccio, *J. Chem. Soc., Dalton Trans.*, 419 (1973).
(8) (a) G. Costa, G. Mestroni, A. Puxeddu, and E. Reisenhofer, *J. Am. Chem. Soc.*, **92**, 2870 (1970); (b) M. J. Carter, D. P. Rillema, and F. Basolo, *ibid.*, **92**, 61 (1970); **96**, 392 (1974); (c) C. K. Chang and T. G. Traylor, *Proc. Natl. Acad. Sci. U.S.A.*, **70**, 2647 (1973).

(9) (a) G. A. Rodley and W. T. Robinson, *Nature (London)*, **235**, 438 (1972); (b) W. T. Robinson, ref 7a, Paper I5.
(10) M. Calligaris, G. Nardin, L. Randaccio, and G. Tauzher, *Inorg. Nucl. Chem. Lett.*, **9**, 419 (1973).
(11) L. D. Brown and K. N. Raymond, *J. Chem. Soc., Chem. Commun.*, 470 (1974), and *Inorg. Chem.*, **14**, 2595 (1975).
(12) R. S. Gall, J. F. Rogers, W. P. Schaefer, and G. G. Christoph, *J. Am. Chem. Soc.*, in press.
(13) R. S. Gall and W. P. Schaefer, in preparation.
(14) R. Sayre, *J. Am. Chem. Soc.*, 77, 6689 (1955).
(15) E. N. Duesler and K. N. Raymond, *Inorg. Chem.*, **10**, 1486 (1971).
(16) S. W. Peterson and H. A. Levy, *Acta Crystallogr.*, **10**, 70 (1957).
(17) A. Avdeef and W. P. Schaefer, to be submitted for publication.
(18) S. C. Abrahams and E. T. Keve, *Acta Crystallogr., Sect. A*, **27**, 157 (1971).
(19) (a) G. Germain, P. Main, and M. M. Woolfson, *Acta Crystallogr. Sect. A*, **27**, 368 (1971); (b) P. Main, M. M. Woolfson, L. Lessinger, G. Germain, and J.-P. Delclercq, "Multan 74, A System of Computer Programmes for the Automatic Solution of Crystal Structures from X-Ray Diffraction Data", University of York, York, England and Laboratoire de Chimie Physique et de Cristallographie, Louvain-la-Neuve, Belgium, Dec 1974.
(20) Most of the computer programs used were from Caltech's CRYM system.[21] The normal probability plots and error analyses were performed with "NORMFSL" and "NORMDP", which are extensions of G. G. Christoph's "NORMAL". A. Avdeef's "METRIC" was used to calculate bond distances and angles along with the associated errors. C. K. Johnson's "ORTEP" program was used for the stereo drawings.
(21) D. J. Duchamp, American Crystallographic Association, Abstracts, Annual Meeting, Bozeman, Mont., 1964, Paper B14.
(22) (a) The function minimized was $S = \sum w(F_o^2 - F_c^2)^2$, where F_o^2 and F_c^2 are the observed and calculated structure factor square-amplitudes and the weights w are taken as $1/\sigma^2(F_o^2)$. Neutral atom scattering factors were used for all of the atoms;[23] (b) GOF (goodness-of-fit) = $[S/(N_o - N_p)]^{1/2}$, $N_o = 6078$ reflections, $N_p = 540$ parameters.
(23) (a) "International Tables for X-Ray Crystallography", Vol. III, The Kynoch Press, Birmingham, England, 1968, p 204; (b) R. F. Stewart, E. R. Davidson, and W. T. Simpson, *J. Chem. Phys.*, **42**, 3175 (1965).
(24) F. L. Hirshfeld and D. Rabinovich, *Acta Crystallogr., Sect. A*, **29**, 510 (1973).
(25) In the final cycle the normal equations matrix was blocked into four parts. The first block contained all of the nonsolvent atomic coordinates, including those of the hydrogen atoms (183 parameters). The second contained all of the nonsolvent anisotropic thermal parameters plus the scale factor (211 parameters). The third contained all of the solvent parameters (108), while the last block contained the 38 isotropic thermal parameters of the hydrogen atom. The maximum non-hydrogen parameter shift-over-error was 0.7 for three of C(3'), which amounted to an atomic shift of 0.005 Å. The maximum hydrogen parameter Δ/σ was 1.1 (H(10)), amounting to a 0.06 Å atomic shift.
(26) This need not be the case if the data were good and the model were poor, as in the case of severe disorder.[27]
(27) A. Avdeef and W. P. Schaefer, *Inorg. Chem.*, **15**, 1432 (1976).
(28) L. Pauling, "The Nature of the Chemical Bond", 3d ed, Cornell University Press, Ithaca, N.Y., 1960, pp 351–352.
(29) A. Earnshaw, P. C. Hewlett, and L. F. Larkworthy, *J. Chem. Soc.*, 4718 (1965).
(30) R. G. Little and J. A. Ibers, *J. Am. Chem. Soc.*, **96**, 4452 (1974).
(31) H. C. Watson, *Prog. Stereochem.*, **4**, 299 (1969).
(32) M. Calligaris, G. Nardin, and L. Randaccio, *Coord. Chem. Rev.*, 7, 385 (1972).
(33) (a) J. W. Lauher and J. A. Ibers, *J. Am. Chem. Soc.*, **96**, 4447 (1974); (b) W. R. Scheidt, *ibid.*, **96**, 90 (1974); (c) R. G. Little, K. R. Dymock, and J. A. Ibers, *ibid.*, **97**, 4537 (1975).
(34) V. Schomaker and K. N. Trueblood, *Acta Crystallogr., Sect. B*, **24**, 63 (1968).
(35) Supplementary material.

Relation between Magnetism and Structure of Iron(III) Complexes Exhibiting an $S = 3/2 \rightleftharpoons S = 5/2$ Spin State Equilibrium. Structures of Chloroform and Water Solvated Tris(4-morpholinecarbodithioato-*S*,*S'*)iron(III) and -manganese(III)

Raymond J. Butcher and Ekk Sinn*

Contribution from the Chemistry Department, University of Virginia, Charlottesville, Virginia 22901. *Received October 20, 1975*

Abstract: The crystal and molecular structures of tris(1-morpholinecarbodithioato-*S*,*S'*)iron(III) crystallized from chloroform (FeM·$CHCl_3$) and toluene (FeM·tol) and the manganese analogue crystallized from chloroform (MnM·$CHCl_3$) were determined by single-crystal x-ray diffraction using computer techniques. Crystal data: FeM·$CHCl_3$, $Fe(S_2CNC_4H_8O)_3$·$CHCl_3$, $P\bar{1}$, $Z = 2$, $a = 9.209$ (4) Å, $b = 10.716$ (4) Å, $c = 14.512$ (9) Å, $\alpha = 101.40$ (6)°, $\beta = 97.02$ (6)°, $\gamma = 90.61$ (6)°, $V = 1392$ Å^3, $R = 4.0\%$, 2934 reflections; MnM·$CHCl_3$, $Mn(S_2CNC_4H_8O)_3$·$CHCl_3$, $P\bar{1}$, $Z = 2$, $a = 13.60$ (1) Å, $b = 11.009$ (5) Å, $c = 11.733$ (5) Å, $\alpha = 117.09$ (4)°, $\beta = 99.89$ (6)°, $\gamma = 107.72$ (5)°, $V = 1387$ Å^3, $R = 4.0\%$, 2576 reflections; FeM·tol, $Fe(S_2CNC_4H_8O)_3$·H_2O, $P\bar{1}$, $Z = 2$, $a = 9.292$ (3) Å, $b = 10.454$ (4) Å, $c = 13.646$ (8) Å, $\alpha = 100.30$ (3)°, $\beta = 95.37$ (4)°, $\gamma = 106.19$ (3)°, $V = 1238$ Å^3, $R = 3.9\%$, 3316 reflections. Like the previously studied dichloromethane solvate, FeM·$CHCl_3$ and FeM·tol exhibit a spin state equilibrium between $S = 3/2$ and $S = 5/2$ states. It now appears that with hydrogen bonding solvates (CH_2Cl_2 in FeM·CH_2Cl_2, $CHCl_3$ in FeM·$CHCl_3$, and H_2O in FeM·tol), the magnetic moment is raised compared to that of the desolvated FeM, and an $S = 3/2$ ground state is produced, whereas FeM shows only $S = 1/2$ and $S = 5/2$ states. A possible mechanism for this, involving solvent hydrogen bonding to ligand sulfur atoms, is discussed. It is likely that $S = 1/2$, $S = 3/2$, and $S = 5/2$ states are all low lying in these and related complexes. In view of this and the extreme solvent sensitivity, many of the earlier literature data for such complexes should be taken with caution. The average metal–ligand bond lengths in the iron complexes increase as the moments increase. ⟨Fe–S⟩ is 2.317 (1), 2.416 (1), 2.430 (4), and 2.443 (1) Å in C_6H_6, $CHCl_3$, CH_2Cl_2, and H_2O solvates, respectively, the latter being the greatest ⟨Fe–S⟩ distance ever observed in a ferric dithiocarbamate. The manganese environment in MnM·$CHCl_3$ exhibits strong tetragonal distortion in addition to the trigonal distortion that occurs in all tris(dithiocarbamate) complexes. Near liquid helium temperature, there is some evidence of the intermolecular antiferromagnetic interaction expected to occur in the manganese and iron complexes, via the electron spin density delocalized onto the ligands.

A large variety of N-substituted ferric dithiochelate complexes lie at or near the high spin ($^6A_1$)–low spin ($^2T_2$) crossover,[1-6] so that their magnetic properties are strongly dependent upon temperature, pressure, substituent groups remote from the metal atoms, and, to a lesser extent, the solvent when in solution. These complexes frequently crystallize with molecules of the recrystallization solvents included in the lattice. Metal–ligand bond lengths alter with variation of the high to low spin ratio, as measured by magnetic properties.[1-3,7,8]

The properties of the complexes then vary with alteration